

Subjective nature of path information in quantum mechanics

Xinhe Jiang^{1,2†}, Armin Hochrainer^{1,2†}, Jaroslav Kysela^{1,2},
Manuel Erhard^{1,2}, Xuemei Gu^{1,3}, Ya Yu^{1,4}, Anton Zeilinger^{1,2*}

¹Institute for Quantum Optics and Quantum Information, Austrian Academy of Sciences, Boltzmanngasse 3, Vienna, 1090, Austria.

²Vienna Center for Quantum Science and Technology, Faculty of Physics, University of Vienna, Boltzmanngasse 5, Vienna, 1090, Austria.

³Max Planck Institute for the Science of Light, Staudtstraße 2, Erlangen, 91058, Germany.

⁴Shanghai Jiao Tong University, Dongchuan Road 800, Shanghai, 200240, China.

*Corresponding author(s). E-mail(s): anton.zeilinger@univie.ac.at;

[†]These authors contributed equally to this work.

Abstract

Common sense suggests that a particle must have a definite origin if its full path information is available. In quantum mechanics, the knowledge of path information is captured through the well-established duality relation between path distinguishability and interference visibility [1–4]. If visibility is zero, a high path distinguishability can be obtained, which enables one with high predictive power to know where the particle comes from. Here we show that this perception of path information is problematic. We demonstrate the simultaneous observation of zero interference visibility and the complete absence of which-path information using a three-crystal interference setup. With a contradictory argument by grouping the crystals in different ways, we show that it is impossible to ascribe a definite physical origin to the photon pair even if the emission probability of one individual source is zero and full path information is available. Our findings shed new light on the physical interpretation of probability assignment and path information beyond its mathematical meaning and reshape our understanding of the whole and part in the context of distinguishability.

Keywords: complementarity principle, visibility, distinguishability, which-way information, duality relation

Introduction

Bohr’s complementarity principle [5] is a cornerstone in quantum mechanics, illustrating the mutual exclusivity of certain properties of a system—such as wave-like interference and particle-like path information. The particle nature is usually characterised by the ability to distinguish between the two paths and to analyse which slit the particle passed through, as famously exemplified by the double-slit interference experiment. Physically, the complementarity principle manifests itself as a question of predictability: could one consistently win with more than 50% probability by betting on the outcome of a which-path measurement? High path distinguishability enables such predictive power but eliminates interference visibility. Conversely, if interference fringes are observed with high visibility, no meaningful path information can be obtained, and outcomes become entirely unpredictable. Quantitatively, the trade-off between the path *distinguishability* (D) (which-way information) and the *visibility* (V) of the interference fringes is encapsulated in the duality relation $D^2 + V^2 \leq 1$ [1–4], indicating that observation of an interference pattern and acquisition of which-way information are mutually exclusive. This duality relation has been extensively studied in two-path interferometers [6, 7].

A striking example of illustrating the duality relation is frustrated down-conversion [8], an interference phenomenon that occurs when photons are generated from two sources [9]. In this setup, photon pairs may be emitted from either crystal, but these two possibilities are aligned so that they overlap perfectly in the spatial and temporal modes. If the two sources are indistinguishable, perfect interference can

occur, but if one source is blocked or misaligned, the photons’ origins become distinguishable and interference is lost. Frustrated down-conversion induces the idea of path identity, which has led to many striking quantum interference effects and quantum applications in recent years [10, 11]. Path distinguishability, in this sense, means the information of which source produced the photon pair. If there is no interference, it is possible to bet on the outcome of a “which-source” measurement that we know with a higher probability of where the photons come from and vice versa. Frustrated down-conversion thus provides a platform to study the interplay between indistinguishability, interference, and which-source information.

The duality relation has also been extended to multi-path interference [12–16]. In such cases, interference between multiple alternative ways of emitting photon pairs can be observed, and these observations have consistently confirmed the duality relation between visibility and distinguishability [17, 18]. In this work, we used a frustrated SPDC system with three nonlinear crystals to explore a different aspect of the duality relation, namely, the interpretation of path information when applying the theoretical formalism to an actual experiment. This stems from the different possibilities of partitioning reality into events that are represented by probability amplitudes. We find that the interpretation of the distinguishability as information about the origin of the photon pairs is inconsistent in a three-crystal setup. Unlike the two-crystal case, ascribing a definite origin to a photon pair is impossible even though full “path information” is available and no interference is observed. This result arises because applying quantum mechanics to the actual system is inherently subjective: There are multiple valid ways to assign probability amplitudes to the events in the experiment, leading to contradictory interpretations of the outcomes. This undermines the view that path information is a definitive and objective property of the system.

Inconsistent which-path information in three-crystal interference

Considering three nonlinear crystals are pumped with the same laser, which emits photon pairs into identical modes (Fig. 1a), the quantum state of the system can be written as [8, 19],

$$|\psi\rangle = ae^{i\phi_A}|s\rangle|i\rangle + b|s\rangle|i\rangle + ce^{i\phi_C}|s\rangle|i\rangle \quad (1)$$

where $ae^{i\phi_A}$, b , $ce^{i\phi_C}$ represent the probability amplitudes of photon pair creation at the respective crystal, $|s\rangle|i\rangle$ represents a signal and idler photon pair in the modes that can be detected, and ϕ_A , ϕ_C are the relative phase between the photons emitted from each crystal pair. The rate of the emitted photon pairs is

$$R(\phi_A, \phi_C) \propto |ae^{i\phi_A} + b + ce^{i\phi_C}|^2 \quad (2)$$

As stated, the amount of “which-source” information and visibility is exclusive due to the complementarity principle. By considering two of the three sources as one single source and applying the duality relation, we show that the analysis of the “which-source” information and visibility from this point of view leads to a contradiction between two possible interpretations of the same experiment.

First, consider the first two nonlinear crystals (NL1 and NL2) to constitute one source labelled by S1, while NL3 constitutes a second source S2, as shown in Fig. 1b. With this treatment, the quantum state of the photon pair in equation (1) can be rewritten as

$$|\psi\rangle = [\alpha + ce^{i\phi_C}]|s\rangle|i\rangle \quad (3)$$

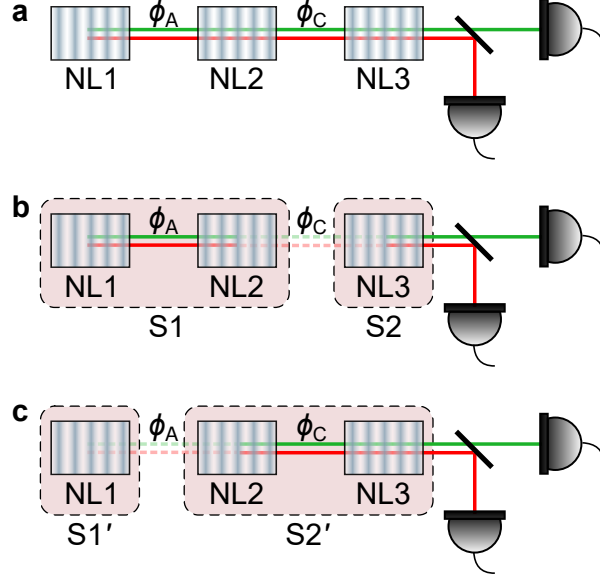


Fig. 1 Schematic of three-crystal interference. a, The three crystals emit photon pairs in identical modes. b, The combination of NL1 and NL2 is considered a single photon pair source (S1). The second source (S2) consists only of NL3. The relative phase ϕ_A between NL1 and NL2 changes the probability of S1 emission. If set to π , the photon pair emission of S1 is completely suppressed. Thus, all emitted photons come from NL3 and no visibility of the total emission rate is observed when varying the relative phase ϕ_C between S1 and S2. c, NL1 corresponds to the source S1', while the combination of NL2 and NL3 is considered a single source S2'. With the same argument, we conclude that all the photons must have originated from NL1 and no visibility is observed when varying the relative phase ϕ_A if $\phi_C = \pi$. These two contradictory situations can be realised in the same experiment when the intensities are balanced and $\phi_A = \phi_C = \pi$. Note that the phase shifter introduces a negative relative phase between NL2 and NL3. Because of its symmetry and periodicity, we represent it as ϕ_C .

where $\alpha = ae^{i\phi_A} + b$ is the probability amplitude corresponding to photon pair emission by S1 and $ce^{i\phi_C}$ corresponds to an emission by S2. Thus, the rate of emitted photons is given by

$$R(\phi_C) \propto |\alpha + ce^{i\phi_C}|^2 \quad (4)$$

Now, we can apply the duality relation between the observed visibility upon varying ϕ_C and the amount of available “source information”. Consider an experimental situation in which $a = b$ and $\phi_A = \pi$. It follows that $\alpha = 0$. Therefore, the probability amplitude corresponding to a pair of photons emitted by S1 is equal to zero.

Thus, S1 is “switched off”. This is consistent with the observation that S1 corresponds to a frustrated down-conversion tuned to completely destructive interference. Consequently, if S2 is removed, in principle, no pair of photons is emitted from the system. However, if instead the first “double” source (S1) is blocked or removed, the photon pair emission rate is unchanged. Therefore, there will be zero interference visibility by varying the relative phase ϕ_C between S1 and S2. These observations are consistent with the duality relation $D^2 + V^2 \leq 1$, as the sources S1 and S2 are unbalanced and the information from “which-source” is available here. One might conclude that all photon pairs come from source S2, that is, from NL3. However, this interpretation leads to a contradiction, as is shown below.

Instead of grouping events into photon-pair emissions from S1 and S2, consider an alternative view of the experiment. Crystal NL1 is considered the first source S1' and the combination of NL2 and NL3 is considered the second source S2', as indicated in Fig. 1c. The possible events are identified accordingly as photon pair emission from either S1' or S2'. In this situation, the quantum state is

$$|\psi\rangle = [ae^{i\phi_A} + \beta] |s\rangle|i\rangle \quad (5)$$

with the probability amplitude for photon pair emission by S1' being $ae^{i\phi_A}$ and the amplitude for S2' is $\beta = b + ce^{i\phi_C}$. The rate of emitted photons is given by

$$R(\phi_A) \propto |ae^{i\phi_A} + \beta|^2 \quad (6)$$

Similarly, we can make the following argument. Taking into account the situation where $b = c$ and $\phi_C = \pi$, it follows that $\beta = 0$. Again, the duality relation $D^2 + V^2 \leq 1$ can be applied in a self-consistent way. Individual blocking of S1' and S2' shows that S2' does not emit photon pairs. In this case, S2' is “switched off”. No interference

visibility will be observed when the phase ϕ_A is varying. This corresponds to full “which-source” information. Thus, we can conclude that the photons were emitted by $S1'$, that is, NL1.

It should be noted that both of these two situations can be realised in one experiment, allowing $a = b = c$ and $\phi_A = \phi_C = \pi$. With this setting, the corresponding rate of detected photons is non-zero and the same for these two situations through equation (2). If we fix one phase to be π and scan another phase, this rate will remain constant, and there will be no interference visibility. At the same time, we still have no information about which crystal produced these photons. We can see that both viewpoints are equally self-consistent and obey the duality relation. However, the interpretations provided by analysing the “which-source” information in two alternative ways of partitioning the system into two separate sources are incompatible with each other.

Experimental demonstration of inconsistent which-path information

The experimental setup is shown in Fig. 2. A 405 nm pump light is used to pump the three periodically poled potassium titanyl phosphate (PPKTP) crystals. The 810 nm photon pairs (signal and idler) are generated in a collinear arrangement through a SPDC process with a type-II configuration. The three crystals emit photons into identical modes. After the third crystal, the pump light is filtered with a dichroic mirror (DM) and a band-pass filter (BPF). Finally, the SPDC photons are detected with single-photon detectors and sent to the coincidence logic for processing. The pump power is low enough so that only one photon pair at a time is present. Phase plates are placed between each pair of crystals and are used to tune the relative phase (ϕ_A and ϕ_C) between the pump, signal, and idler photons. The lenses between each

pair of crystals form 4f systems to obtain good spatial overlap of the SPDC photons from each crystal.

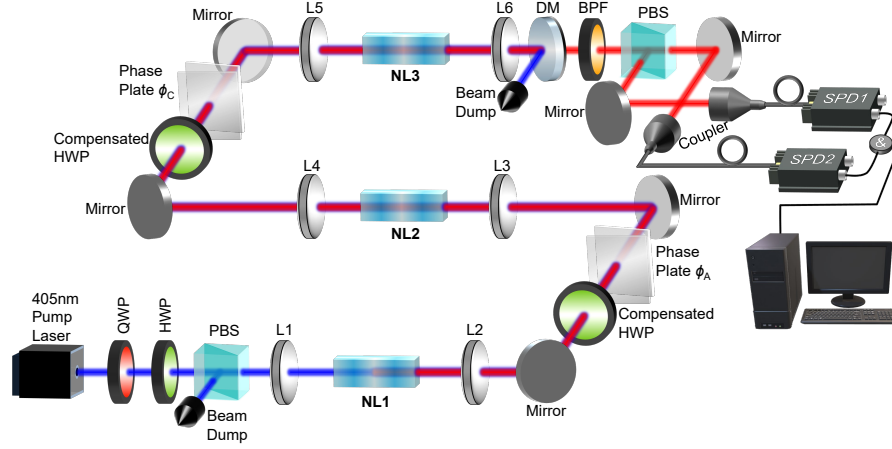


Fig. 2 Experimental setup of the three-crystal interference. The 405 nm pump laser is used to pump the three crystals. The SPDC photons are generated and emitted in identical modes. Each crystal is enclosed by two lenses, and one pair of crystals forms a 4f system. This ensures that the first crystal is imaged onto the second crystal and a good spatial overlap of the beams created in the two SPDC processes is obtained. The phase plates between each pair of crystals are used to change the relative phases (ϕ_A and ϕ_C) of the pump, signal, and idler photons. To compensate for the longitudinal walk-off caused by the different group velocities of signal and idler photons, we used two compressed half-wave plates between each pair of crystals. The photons are finally filtered and collected in the fibre for coincidence counts. QWP: quarter-wave plate. HWP: half-wave plate. PBS: polarising beam splitter. NL1-NL3: Nonlinear crystals 1-3. L1-L6: lenses 1-6. DM: dichroic mirror. BPF: band-pass filter. SPD: single-photon detector. &: coincidence logic.

To obtain good interference visibility between all crystals, the spectral and spatial degrees of freedom of the SPDC photons should be indistinguishable. This can be realised with identical crystals and by overlapping their spatial mode through fine-tuning the position of lenses in the setup. To facilitate this, we used an ICCD camera to image the SPDC photons. The lens system allows us to successively image signal and idler beams originating from each of the SPDC processes at the crystal and at its Fourier plane. The photon beams from the three SPDC processes are aligned to overlap in both planes to ensure that they are indistinguishable in any plane. The details and characteristics of the imaging are shown in the Methods, ‘Characterization

of SPDC photons'. In addition, the crystal temperature is also optimised to ensure a degenerate photon pair emission from all three crystals.

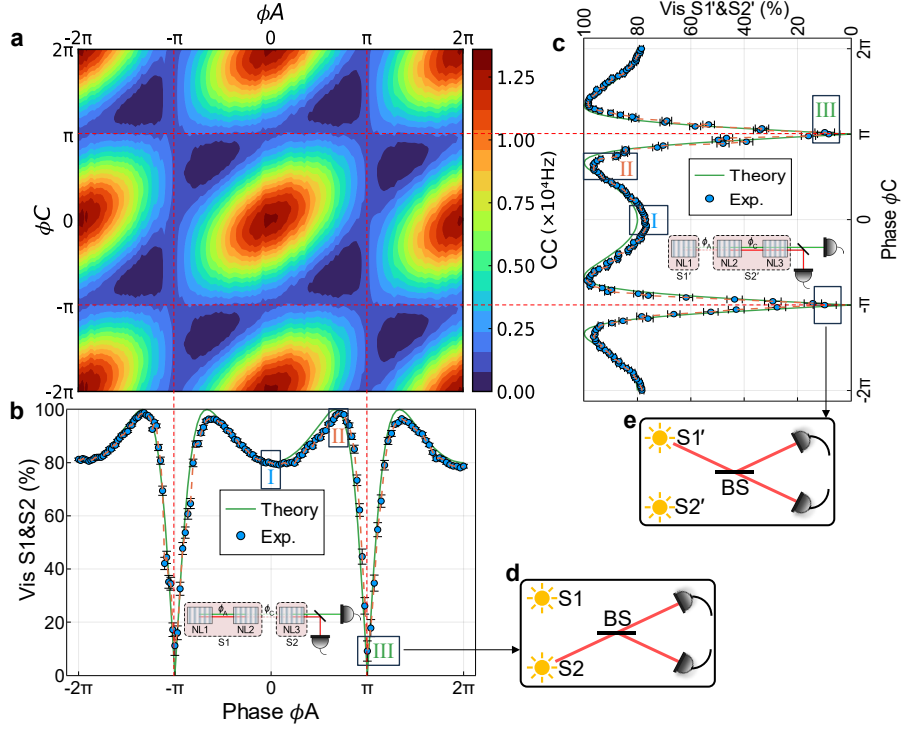


Fig. 3 Three-crystal interference obtained with a 2D scan. a, Contour plot shows the detected coincidence counts (CC) when all three crystals are active upon varying both phases ϕ_A between NL1 and NL2, and ϕ_C between NL2 and NL3. b, Visibility observed between S1 and S2 when each phase ϕ_A is fixed and phase ϕ_C is scanned. Inset shows the first picture which regard the system as a two path interferometer between S1 and S2. At the phase point $\phi_A = (2k + 1)\pi$ ($k \in \mathbb{Z}$), the photon pair emission from S1 is suppressed, as shown schematically in d. c, Visibility observed between S1' and S2' when each phase ϕ_C is fixed and phase ϕ_A is scanned. Inset shows another picture which regard the system as two path interferometer between S1' and S2'. In an analogous manner, the photon pair emission from S2' is suppressed at phase point $\phi_C = (2k + 1)\pi$ ($k \in \mathbb{Z}$), as shown schematically in e. The coincidence count data in frames I, II, III of b,c are shown in Fig. 4a,b, respectively. The green line in b and c is the theoretical prediction. The blue dot is the experimental data. The dashed orange line is a guide for the eye. BS: Beam splitter.

To get a full view of how visibility changes when one phase is fixed and the other phase is scanned, we set different values for one phase and obtain visibility by scanning the other phase, as shown in Fig. 3. As it is periodic, only some periods are given. Figure 3a shows the contour plot when all three crystals are active and the two phases

are varied. For comparison, the theoretical contour plot is given in Extended Data Fig. 1b. First, phase ϕ_A is set to different values and the visibility is calculated when phase ϕ_C is scanned (see Fig. 3b). As can be seen, visibility is highest when the phase is set to $\phi_A = 2\pi/3$. This is because the amplitude of the combination of NL1 and NL2 is more balanced compared to the amplitude of NL3 at this point. They have better interference visibility as a result of their better indistinguishability. However, at the point $\phi_A = \pi$, they show almost no interference due to complete distinguishability. Similar results are also obtained when the phase ϕ_C is set to different values and the visibility is measured by scanning the relative phase ϕ_A (see Fig. 3c). The inset of Fig. 3b,c shows the two pictures when the crystals are grouped differently. At the phase point $(2k + 1)\pi$ ($k \in \mathbb{Z}$), the photon pair emission is suppressed, corresponding to one of the sources (S1 or S2') being switched off in the two-source interferometer, as shown schematically in Fig. 3d,e. Therefore, the knowledge that photons can only be emitted by the other source (S2 and S1') yields full interferometric path information in the sense that one could always win a bet on the outcome of the measurement on the individual sources.

In Fig. 4a,b, we plot the interference fringe at three representative phases 0, $2\pi/3$ and π , which are labelled I, II and III in Fig. 3b,c. Phase 0 has higher counts but lower visibility. Phase $2\pi/3$ has lower counts, but the highest visibility. Phase π exhibits almost no visibility. More theoretical analysis and comparison with experimental data can be found in Methods. To take a closer look at these two pictures, one of the phases is fixed as π , and the other phase is scanned. According to the theoretical analysis, we will see a constant count rate. In our experiment, the visibilities of the interference between S1 and S2 and between S1' and S2' when setting $\phi_A = \pi$ and $\phi_C = \pi$ are $9.12 \pm 3.81\%$ and $8.30 \pm 4.19\%$, respectively. This is almost close to the random noise level when there is no interference at all. In Fig. 4c,d, we plot the coincidence counts (CC) with error bars when $\phi_A = \pi$ and $\phi_C = \pi$, respectively. It can be seen that CC

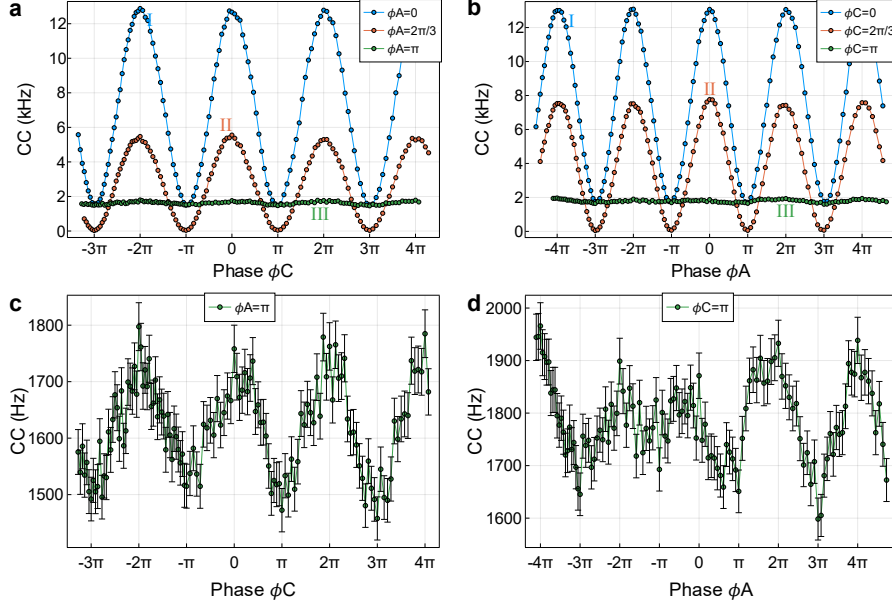


Fig. 4 Interference fringes at the phase point 0, $2\pi/3$, and π . a,b, Coincidence counts (CC) for the three points I: $\phi_A = 0$ ($\phi_C = 0$), II: $\phi_A = 2\pi/3$ ($\phi_C = 2\pi/3$), III: $\phi_A = \pi$ ($\phi_C = \pi$) chosen in Fig. 3b,c, respectively. c, CC versus ϕ_C when relative phase $\phi_A = \pi$. d, CC versus ϕ_A when relative phase $\phi_C = \pi$. The lines are guides to the eye. Errors are determined by assuming Poissonian counting statistics.

fluctuates within a small range. This even reaches the random noise level. In addition, the two cases have overlapping count regions (1600-1800 Hz). In this region, we cannot tell at all from which crystal the photons come. Using the counts data, we estimate that the path information corresponds to photon pairs originating from NL3 with the probability $p_3 = 95.14 \pm 0.59\%$ when $\phi_A = \pi$ and from NL1 with the probability $p_1 = 96.41 \pm 0.47\%$ when $\phi_C = \pi$ (the probability is calculated by CC_{NL1}/CC_{tot} and CC_{NL3}/CC_{tot} , where $CC_{NL1} = CC_{tot} - CC_{S2'}$ and $CC_{NL3} = CC_{tot} - CC_{S1}$, $CC_{S1}/CC_{S2'}$ are counts when crystal NL3/NL1 is off and the phases are set to π , CC_{tot} are the counts when all three crystals are on and the phases are set to π). As $p_1 + p_3 > 1$, we arrive at a contradiction because it is impossible to have a probability larger than 1 in an experiment carried out with $\phi_A = \phi_C = \pi$. It should be noted that it is not possible to have equal overlapping regions and a constant count because of the experimental imperfections. Therefore, visibility cannot completely become zero

at phase π . The analysis of some of the experimental errors is shown in Methods, ‘Optimisation of the visibility’.

Discussion and conclusion

Note that in a periodically poled crystal, the amplitudes of pair creations at different crystal sections are engineered to interfere constructively to increase the pair-creation efficiency. Usually, a single probability amplitude is assigned to photon pair emission within the whole crystal, but no description is given anymore at which position inside the crystal the photon originates. In an analogue fashion, we can also group two crystals together and assign a single probability amplitude for the photon pair emission. However, the assignment of a probability amplitude of zero to an event should not be interpreted as a zero probability that this event will occur. In the experiment of frustrated down-conversion [8], ideally no photon pairs are detected if there is complete destructive interference between two photon-pair emission processes. Nevertheless, the possibility for a photon pair originating from frustrated down-conversion cannot be ruled out if a third nonlinear crystal were inserted before the detectors. Therefore, a measured probability of zero for an isolated subsystem does not mean that this probability remains zero in the presence of other subsystems [19], since all subsystems can interfere with each other.

Another interesting point is to realise the subtle difference in the meaning of the “which-way information” depending on what measurement is performed [19]. If the three crystals are analysed separately, “which-way information” refers to the question “which crystal generates the photons before they arrived at the detectors”. If two of them are grouped together and assigned one common probability amplitude, the “which-way information” then corresponds to the question “which of the two possible events happened? Did the photons come from the first crystal or from a combination of the other two?” Despite these different perspectives, the amount of path information

remains entirely dependent on visibility via the duality inequality. Therefore, in the situation of both phases set to π , all these pictures are equally valid and self-consistent, although they lead to contradictory which-way information.

Bohr’s complementarity principle is usually understood as the wave-particle duality relation. The visibility of an interference pattern is used to quantify the wave property, and the path information is used to quantify the particle property. The one-particle and two-particle interference are widely characterized in the framework of the duality relation. This interference phenomenon has its roots in the fundamental indistinguishability of identical quantum particles. In single and two-particle interferometry, this complementarity is explored through the relationship between path distinguishability and the visibility of interference fringes [1, 3, 20–22]. Compared with two-particle interference, there exist entirely different implications in the three-particle interferometry that are worth further investigation [23]. Our experiment also demonstrates one important feature of quantum mechanics: the description of the quantum system must encompass all the possible outcomes, as long as no intervention is made to make the parts distinguishable in principle. Whether the quantum system should be treated as a whole or as separable parts depends on whether the parts can be distinguished from each other. This point of view may renovate our understanding of the interplay between whole and part in the context of distinguishability.

In this work, we showed that both no which-way information and no interference could be realised in one experiment by involving three indistinguishable sources. By considering two of the three sources as a single source, two contradictory interpretations of the path information are possible within the experimental configuration. This brings about a refinement of the meaning of “which-way information”. Usually, we identify macroscopically distinguishable “events” and assign probability amplitudes to them. However, this identification of “events” is generally ambiguous. Any event could in principle be subdivided into subevents of non-zero probability amplitude,

which can lead to a zero probability amplitude of the combined event. Therefore, the “which-way information” can only be meaningfully defined if the context is clarified and the events are explicitly specified in this context. Our findings suggest that path information depends not only on the physical system, but also on how to translate the formula to an actual experiment. This offers a fresh perspective on quantum interference. By revealing the subtleties of frustrated down-conversion in multi-crystal setups, this work deepens our understanding of quantum phenomena and raises important questions about the nature of path information in quantum mechanics.

References

- [1] Greenberger, D. M. & Yasin, A. Simultaneous wave and particle knowledge in a neutron interferometer. *Phys. Lett. A* **128**, 391–394 (1988).
- [2] Herzog, T. J., Kwiat, P. G., Weinfurter, H. & Zeilinger, A. Complementarity and the quantum eraser. *Phys. Rev. Lett.* **75**, 3034–3037 (1995).
- [3] Jaeger, G., Shimony, A. & Vaidman, L. Two interferometric complementarities. *Phys. Rev. A* **51**, 54–67 (1995).
- [4] Englert, B.-G. Fringe visibility and which-way information: An inequality. *Phys. Rev. Lett.* **77**, 2154–2157 (1996).
- [5] Bohr, N. The quantum postulate and the recent development of atomic theory. *Nature* **121**, 580–590 (1928).
- [6] Dürr, S., Nonn, T. & Rempe, G. Fringe visibility and which-way information in an atom interferometer. *Phys. Rev. Lett.* **81**, 5705–5709 (1998).
- [7] Abranyos, Y., Jakob, M. & Bergou, J. Interference and partial which-way information: A quantitative test of duality in two-atom resonance. *Phys. Rev. A* **61**,

013804 (1999).

- [8] Herzog, T. J., Rarity, J. G., Weinfurter, H. & Zeilinger, A. Frustrated two-photon creation via interference. *Phys. Rev. Lett.* **72**, 629–632 (1994).
- [9] Pfleegor, R. L. & Mandel, L. Interference of independent photon beams. *Phys. Rev.* **159**, 1084–1088 (1967).
- [10] Hochrainer, A., Lahiri, M., Erhard, M., Krenn, M. & Zeilinger, A. Quantum indistinguishability by path identity and with undetected photons. *Rev. Mod. Phys.* **94**, 025007 (2022).
- [11] Krenn, M., Hochrainer, A., Lahiri, M. & Zeilinger, A. Entanglement by path identity. *Phys. Rev. Lett.* **118**, 080401 (2017).
- [12] Dürr, S. Quantitative wave-particle duality in multibeam interferometers. *Phys. Rev. A* **64**, 042113 (2001).
- [13] Zawisky, M., Baron, M. & Loidl, R. Three-beam interference and which-way information in neutron interferometry. *Phys. Rev. A* **66**, 063608 (2002).
- [14] Bimonte, G. & Musto, R. On interferometric duality in multibeam experiments. *Journal of Physics A: Mathematical and General* **36**, 11481 (2003).
- [15] Englert, B.-G., Kaszlikowski, D., Kwek, L. C. & Chee, W. H. Wave-particle duality in multi-path interferometers: General concepts and three-path interferometers. *Int. J. Quantum Inf.* **06**, 129–157 (2008).
- [16] Asad Siddiqui, M. & Qureshi, T. Three-slit interference: A duality relation. *Progress of Theoretical and Experimental Physics* **2015**, 083A02 (2015).

- [17] Heuer, A., Menzel, R. & Milonni, P. W. Complementarity in biphoton generation with stimulated or induced coherence. *Phys. Rev. A* **92**, 033834 (2015).
- [18] Heuer, A., Menzel, R. & Milonni, P. W. Induced coherence, vacuum fields, and complementarity in biphoton generation. *Phys. Rev. Lett.* **114**, 053601 (2015).
- [19] Hochrainer, A. *Path Indistinguishability in Photon Pair Emission*. Ph.D. thesis, University of Vienna (2020).
- [20] Horne, M. A., Shimony, A. & Zeilinger, A. Two-particle interferometry. *Phys. Rev. Lett.* **62**, 2209–2212 (1989).
- [21] Jaeger, G., Horne, M. A. & Shimony, A. Complementarity of one-particle and two-particle interference. *Phys. Rev. A* **48**, 1023–1027 (1993).
- [22] Abouraddy, A. F., Nasr, M. B., Saleh, B. E. A., Sergienko, A. V. & Teich, M. C. Demonstration of the complementarity of one- and two-photon interference. *Phys. Rev. A* **63**, 063803 (2001).
- [23] Greenberger, D. M., Horne, M. A. & Zeilinger, A. Multiparticle Interferometry and the Superposition Principle. *Phys. Today* **46**, 22–29 (1993).
- [24] Lee, S. M., Kim, H., Cha, M. & Moon, H. S. Polarization-entangled photon-pair source obtained via type-ii non-collinear spdc process with ppktp crystal. *Opt. Express* **24**, 2941–2953 (2016).

Methods

Theoretical analysis

In this section, we present more theoretical results of the three-crystal interference. As stated in the main text, the rate of the emitted photon pairs can be calculated

through the equation (2). Assuming that the three crystals emit photons of the same amplitude, that is, $a = b = c = 1$, the count rate can be obtained when varying the two phases. The count rate versus the phases ϕ_A and ϕ_C is shown in Extended Data Fig. 1. Note that at the point $\phi_A = \phi_C = \pi$, there is a non-zero photon pair emission rate with zero visibility.

The cross section for different phases ϕ_A is shown in the Extended Data Fig. 2. Due to symmetry, the result is the same for phase ϕ_C . We choose several representative points to see how the visibility changes with the phases. We can see that the visibility is highest at the point $2\pi/3$ and becomes zero at the point π . The counts of $\pi/3$ ($2\pi/3$) and $5\pi/3$ ($4\pi/3$) are symmetric with respect to $\phi = \pi$. Therefore, they show the same visibility. To compare them, the minimum (maximum) point of the experimental data is aligned at π ($2\pi/3$) in the main text (Fig. 3). Due to periodicity, the two points $\phi_A = 0$ and $\phi_A = 2\pi$ overlap each other. One feature is that the minimal and maximal counts at the middle phase point (e.g. $\phi_A = \pi/3$) are higher than at the lowest visibility point (i.e. $\phi_A = \pi$). To have a comprehensive comparison, we again show the visibility during the period from -2π to 2π in Extended Data Fig. 3. Theoretically, the visibility is 0 at phase π and 1 at phase $2\pi/3$. The visibility is 80% when the relative phase is 0.

Characterization of SPDC photons

To guarantee that the SPDC photons from the three crystals have a good spatial overlap, we placed crystals one by one and imaged the SPDC photons with an ICCD camera. The setup of the imaging system is shown in Extended Data Fig. 4. This system allows for successive images of both SPDC processes at the crystal and at its Fourier plane. Without L7 in place, the lenses L2, L3, and L6 map the Fourier plane of the crystals to the camera plane. If the lens L7 is inserted, the two lenses after each crystal make up an imaging system that produces an image of the crystal in the camera. Therefore, the photons from the SPDC processes of each crystal are aligned

to overlap in both planes, which ensures their indistinguishability in any plane. After this alignment, the lens system and camera are removed from the setup using a flip mirror (FM). The images of the SPDC photons from the three crystals are shown in Extended Data Fig. 5. We can see that they are almost the same size both at the Fourier plane and at the crystal plane after a good alignment.

The interference visibility between each pair of crystals is first optimised in the experiment. The results are shown in Extended Data Fig. 6. The visibility is quantified by $Vis = (CC_{Max} - CC_{Min}) / (CC_{Max} + CC_{Min})$, where CC is the coincidence count rate. After recursive optimisation, the observed visibility between NL1 and NL2 is $98.53 \pm 0.18\%$ and the visibility between NL2 and NL3 is $98.68 \pm 0.17\%$. This indicates that each pair of crystals exhibits a high degree of coherence.

Note that the spectral and spatial distributions of the SPDC photons from the PPKTP crystal are correlated. Both are influenced by the pump wavelength, the bandwidth of the band-pass filter, and the crystal temperature. To graphically illustrate the phenomena, we schematically plot the angle distribution of the SPDC photons versus the wavelength at different crystal temperatures, as shown in Extended Data Fig. 7a. The filter for different bandwidths is also plotted. One observation is that the SPDC photons appear to be located in a ring when the temperature is low. It then becomes a spot as the temperature increases. The narrower the bandwidth of the filter, the higher the temperature it needs for the photons at the centre to appear. The image measured with the temperature change is shown in Extended Data Fig. 7b-g. These results are consistent with previous work [24]. Usually, we need to adjust the temperature at which the SPDC photons at 0° just appear within the bandwidth, for example, the curve of temperature T_3 in Extended Data Fig. 7a. This can ensure that the photons have a good collinear overlap. The intersection point of the H and V photons is the degenerate point, which is at the double of the pump wavelength. In the experiment, it is hard to adjust the central wavelength of the band-pass filter and the

degenerate point to be the same. This will cause asymmetry of the H and V photons. When the H- and V-photons exchange the roles with the compensated HWP between each pair of crystals, the photons from the two crystals will have some distinguishability because of this asymmetry. This is one of the sources of errors that cause visibility degradation.

Comparison of experimental and theoretical data

In the main text, we compare the experimental and theoretical visibility for the 2D scan. Here, we calculate the theoretical counts when one phase is fixed and the other phase is scanned, and compare it with our experimental data. For simplicity, we pick up three representative points, that is, 0, $2\pi/3$, and π . The counts versus the phase are shown in the Extended Data Fig. 8. We can see that the visibility at phase $2\pi/3$ is the highest, i.e., 1 in theory. The visibility at phase π is 0 in theory. The visibility at phase 0 is 80% in theory. Our experimental data are in good agreement with the prediction of the theory.

Optimisation of the visibility

In the experiment, the SPDC photons must have a good spatial and spectral overlap to have a good indistinguishability. The spatial overlap can be easily realised by imaging the photons and adjusting the lens system and the translation and tilt of the crystals. To have a good spectral overlap, we use a band-pass filter. Some unwanted photons, which cause the distinguishability, can also be filtered with a single-mode fibre. In addition, the crystal temperature also needs to be optimised back and forth. To ensure coherent emission of these crystals, the optical path-length difference (OPLD) should also meet some requirements. One is that the OPLD between the pump beam and the two down-converted photons must be smaller than the coherence length of the pump

laser [10],

$$|(L_{P_i} + L_{\text{SPDC}_i}) - (L_{P_j} + L_{\text{SPDC}_j})| \underset{(i,j) \in \{1,2,3\}}{\overset{i \neq j}{\leq}} L_{\text{P}}^{\text{coh}} \quad (7)$$

where $L_{P_{i/j}}$ are the optical path length of the pump beam from the pump laser to each crystal, $L_{\text{SPDC}_{i/j}}$ represent the optical path length of the respective down-converted photons from each crystal to the detector, and $L_{\text{P}}^{\text{coh}}$ denotes the coherence length of the pump laser. Another condition is that the OPLD of the down-converted photons should be less than their coherence length,

$$|(L_{S_j} - L_{I_j}) - (L_{S_i} - L_{I_i})| \underset{(i,j) \in \{1,2,3\}}{\overset{i \neq j}{\leq}} L_{\text{SPDC}}^{\text{coh}} \quad (8)$$

with $L_{S_{i/j}}$ representing the optical path length of the signal photons from each crystal to the detector and $L_{I_{i/j}}$ for idler photons, $L_{\text{SPDC}}^{\text{coh}}$ denoting the coherence length of the down-converted photons. The first condition is easy to fulfill. To fulfill the second condition, we placed a compensated half-wave plate in the path. This wave plate is used to exchange the polarisation of the signal and idler photons and to compensate for the longitudinal walk-off between them. This will make their OPLD within the coherence length of the down-converted photons.

The general procedure of optimisation is first to adjust the coupling to get the maximal coincidence counts from the first crystal. The second crystal then opens. The SPDC efficiency is adjusted by tilting and moving the position of the crystal. The purpose is to make the counts of the two crystals as equal as possible. Then the phase between the two crystals is scanned. The temperature of the crystals is tuned to maximise their interference visibility. In addition, the relative position of the two crystals is tuned to further improve visibility. The third crystal is opened after a good visibility for the first two crystals is obtained. Meanwhile, the first crystal is closed.

Then, the position and temperature of the third crystal are optimised to maximise the visibility of the last two crystals. To keep the visibility of the first two crystals, the second crystal is not touched. After good visibility is obtained, we return to the first two crystals. The second crystal is adjusted to ensure that both pairs have good visibility. This procedure is repeated many times until we get good visibility on both sides. The phase is very sensitive to air fluctuations and mechanical vibration. To stabilise the phase, we isolate the setup with a box. After this, we can do a 2D scan in the long run.

One thing is that visibility degrades over time. This is caused by some residual strain on the mount stages of each optical component. Note that any small disturbance can induce a change in the spatial position of the SPDC beams and thus lead to the distinguishability of the SPDC photons from each crystal. Based on the theoretical model, all the errors that degrade visibility can be ascribed to three cases, namely the longitudinal misalignment, the transversal misalignment, and the tilt of each optical component. We have an estimation of these errors using relation $V^2 + D^2 = 1$ and define the quantity D as any non-overlap portion of the beam which leads to the distinguishability. The visibility degradation caused by these errors is shown in Extended Data Fig. 9. The transversal and tilt errors have the most important influence on the visibility. Because the beam size is focused at about $50 \mu m$, any transversal deviation at this scale will cause a great reduction in visibility. The tilt error will be magnified with the propagation distance. As shown in Extended Data Fig. 9a, the two beams overlap at position 1 and deviate from each other with a tilt angle θ . After distance L , they are fully distinguishable. With a realistic propagation distance of 400 mm between the two crystals, we get the variation of visibility versus the tilt angle. For our setup, the beams propagate longer distances before they are collected in the fiber. A 0.1° tilt will reduce visibility to 97%. Therefore, we must carefully optimise the position and tilt of each optical component and crystal.

Another factor that influences visibility is the photon yield imbalance. This is because the pump power of each crystal cannot be the same because of the non-unity transmission of each optical component between the crystals. Assume that the photon yields of NL1, NL2, and NL3 are A , B , and C , respectively. The ideal case is $B/A = 1$ and $C/A = 1$. We theoretically analyse the photon yield imbalance error, which is shown in Extended Data Fig. 10. We can see that the error has a significant influence on the phase points of π and 0. With an imbalance of 0.9, the visibility at phase π has already deviated from the ideal value of 0 to 10%. Based on our measurement, the photon yield is approximately $A = 2200$ Hz, $B = 2000$ Hz, and $C = 1800$ Hz for each individual crystal. By substituting these experimental values, our visibility shows good agreement with the theoretical results taking these realistic errors into account.

Data availability

The data presented in the figures within this paper and other findings of this study are available from the corresponding authors upon reasonable request.

Acknowledgements

We would like to thank R. Kindler for the helpful discussions. This work was supported by the Austrian Academy of Sciences, the European Research Council (Simulators and Interfaces with Quantum Systems [SIQS] Grant 600645 EU-FP7-ICT), the Austrian Science Fund: F40 (Special Research Programmes [SFB] Foundations and Applications of Quantum Science [FoQuS]) and W 1210-N25 (Complex Quantum Systems [CoQuS]), and the University of Vienna via the QUESS project (Quantum Experiments on Space Scale).

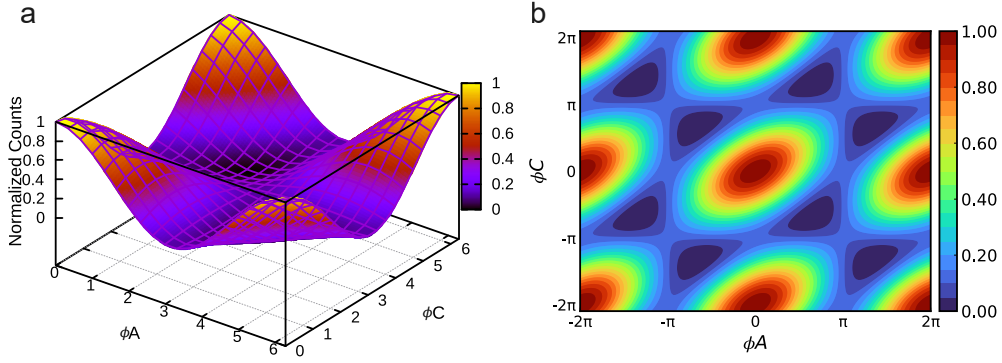
Author contributions

X. J., A. H., J. K. and M. E. carried out the experiment. X. J. collected the data with assistance from J. K., X. G. and Y. Y.. X. J. and A. H. analysed the data and performed the numerical calculations. X. J. wrote the paper with the input of all other authors. A. H. and A. Z. conceived the project. A. Z. supervised the research. All authors discussed the experimental results.

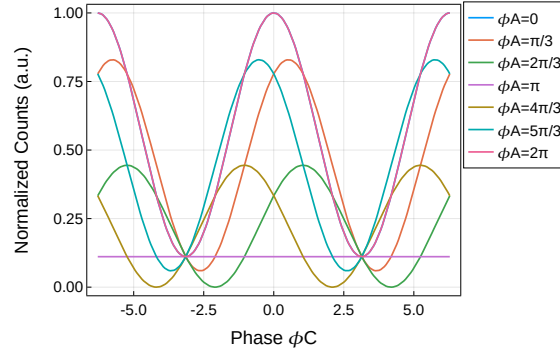
Competing interests

The authors declare no competing interests.

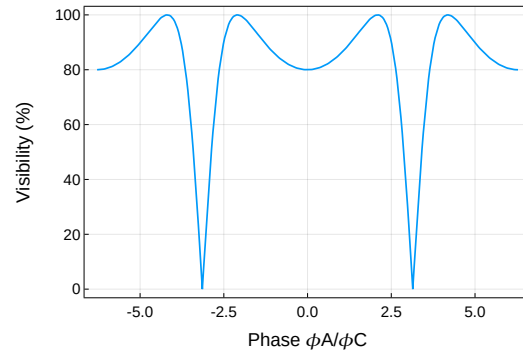
Extended Data



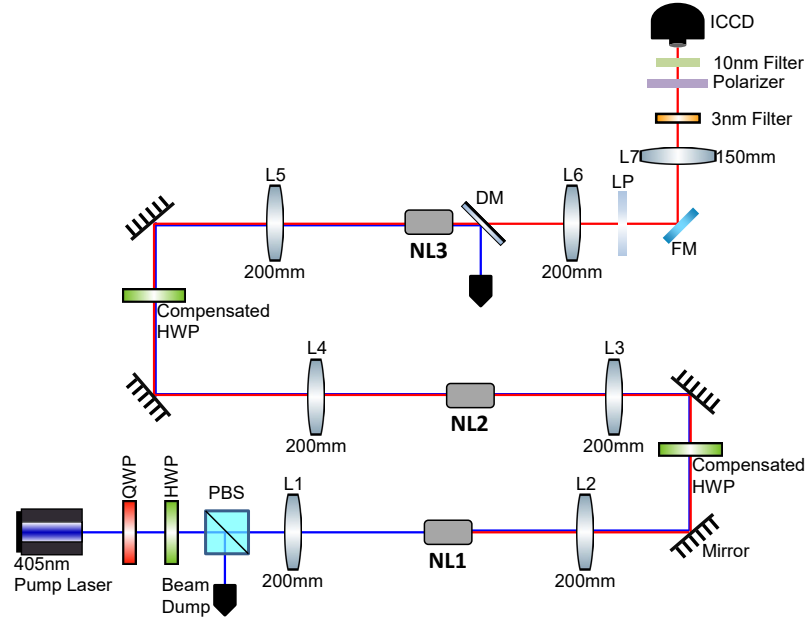
Extended Data Fig. 1 a, Count rates on varying phase ϕ_A and ϕ_C obtained with equation (2). The range is from 0 to 2π . b, Theoretical contour plot in the range from -2π to 2π . Equal emission probabilities a , b , and c are assumed. At the point $\phi_A = \pi/\phi_C = \pi$, we can see that there is no interference visibility.



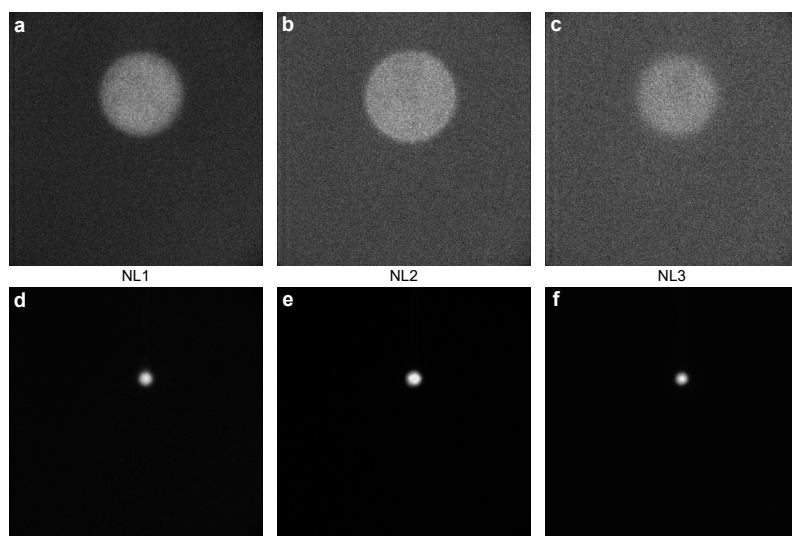
Extended Data Fig. 2 Count rates versus phase ϕ_C for several fixed phases $\phi_A = 0, \pi/3, 2\pi/3, \pi, 4\pi/3, 5\pi/3, 2\pi$. Note that the highest visibility curve has a lower count rate and the middle visibility curve has a higher count rate.



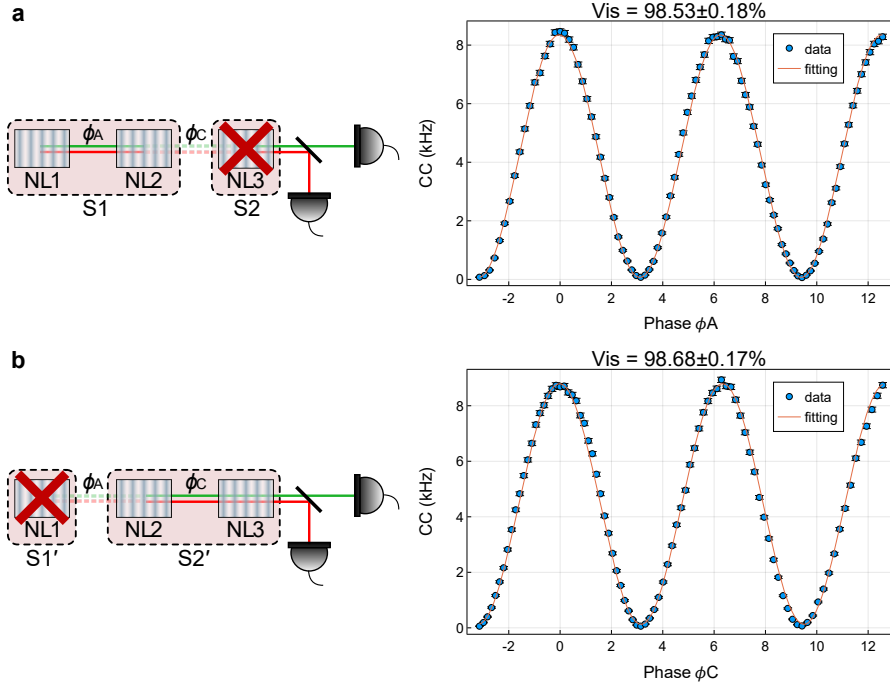
Extended Data Fig. 3 Interference visibility between the three crystals. The range is from -2π to 2π . Three particular points are interesting for us to compare, i.e., phase 0, phase $2\pi/3$ of highest visibility 1, and phase π of zero visibility.



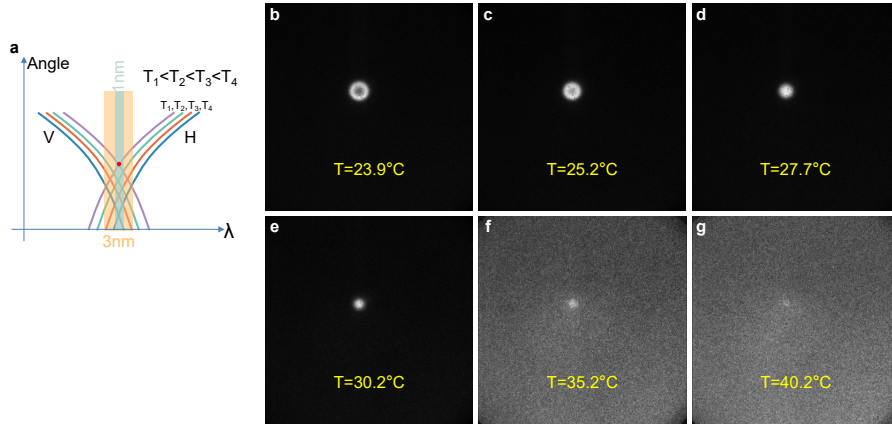
Extended Data Fig. 4 Setup for the imaging of the SPDC photons from the three crystals. The setup before the flop mirror (FM) is almost the same as in the main text; only the phase plate is not included. After FM, we used an imaging system to image the SPDC photons on the ICCD camera.



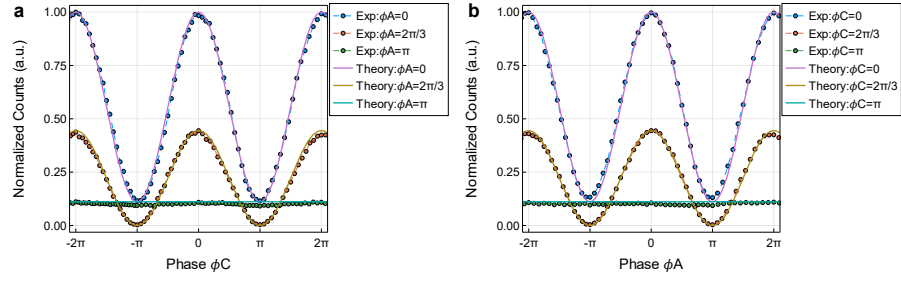
Extended Data Fig. 5 Image of the SPDC photons from the three crystals with an ICCD camera.



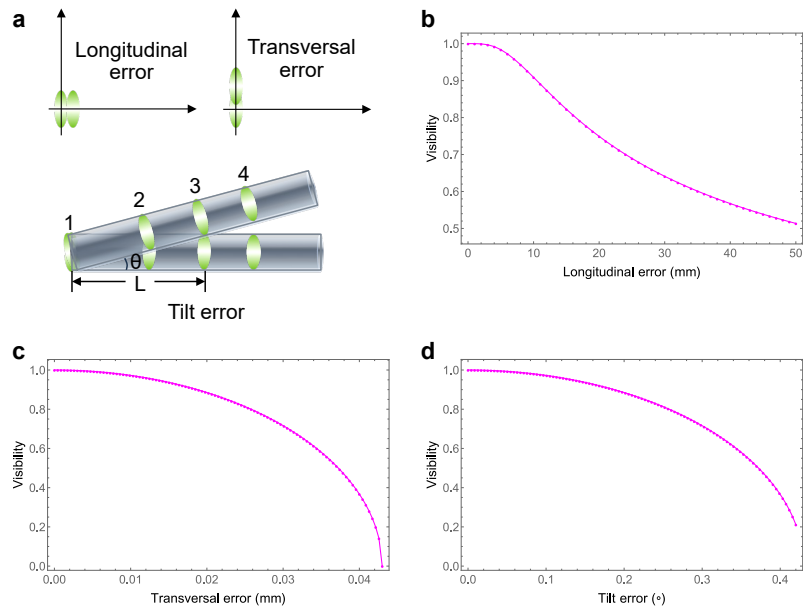
Extended Data Fig. 6 Interference between each pair of crystals. a, Left: Grouping of NL1 and NL2. Right: Coincidence counts (CC) versus relative phase ϕ_A when NL3 is blocked. The interference visibility obtained between NL1 and NL2 is $98.53 \pm 0.18\%$. b, Left: Grouping of NL2 and NL3. Right: CC versus the relative phase ϕ_C when NL1 is blocked. The interference visibility obtained between NL2 and NL3 is $98.68 \pm 0.17\%$. The data are fitted with a sinusoidal curve. Errors are determined by assuming Poissonian counting statistics.



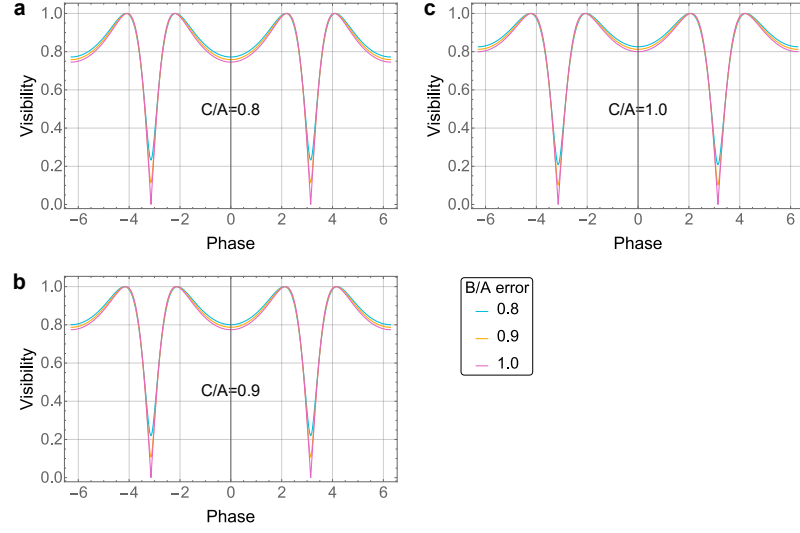
Extended Data Fig. 7 a, Angle distribution of the SPDC photons versus the wavelength at different crystal temperatures. This is an ideal case. Normally, the central wavelength of the band-pass filter is not the same as the degenerate wavelength of the SPDC photons. In addition, the photons at 0° angle are not within the bandwidth of the filter. Therefore, we usually collect photons located at the rings filtered by the band-pass filter. b-g, Variation of the SPDC beam spot when changing the crystal temperature. In the experiment, the crystal temperature is optimised around 30°C .



Extended Data Fig. 8 Count rate versus the phase ϕ_C (a) and phase ϕ_A (b). For comparison, the experimental counts are normalised with respect to the corresponding theoretical maximum.



Extended Data Fig. 9 Visibility degradation caused by three different kinds of alignment errors. a, Schematic of the three errors. b, Visibility versus longitudinal error. c, Visibility versus transverse error. d, Visibility versus the tilt error.



Extended Data Fig. 10 Visibility deviation due to the photon yield imbalance of the three crystals. a, b and c are for the different imbalance ratios C/A between NL3 and NL1. The three lines in each figure correspond to the different imbalance ratios $B/A = 0.8, 0.9, 1.0$ between NL2 and NL1, as shown in the legend. Here, the abscissa is the phase ϕ_A . The results are the same for phase ϕ_C .